



MINISTRY OF SUPPLY

AERONAUTICAL RESEARCH COUNCIL
REPORTS AND MEMORANDA

The Flutter Properties of a Simple Aero-isoclinic Wing System

By

N. C. LAMBOURNE, B.Sc. and A. CHINNECK,
of the Aerodynamics Division, N.P.L.

Crown Copyright Reserved

LONDON : HER MAJESTY'S STATIONERY OFFICE

1956

PRICE 4s. 6d. NET

The Flutter Properties of a Simple Aero-isoclinic Wing System

By

N. C. LAMBOURNE, B.Sc. and A. CHINNECK,
of the Aerodynamics Division, N.P.L.

*Reports and Memoranda No. 2869**

January, 1950

Summary.—The work dealt with in this report is of an exploratory nature primarily intended to provide some understanding of the flutter characteristics of a Hill aero-isoclinic wing. Essentially, this is a swept-back wing elastically designed so that the lifting loads do not affect the aerodynamic incidence. The aero-isoclinic property is dependent on the change of incidence due to torsion of the wing being neutralised by that produced by wing bending. The simple aero-isoclinic system used in the tests consisted of a rigid aerodynamic lifting surface having the two essential freedoms, rotation about a swept-back axis, and rotation about a perpendicular axis at the root. Flutter critical speeds and frequencies were measured over a range of the ratio of the bending and torsion frequencies; the results show that the aero-isoclinic condition is not sufficient to prevent flutter, and further that the critical speed for flutter may be low. As usual, forward mass-loading of the wing raises the critical speed.

A subsidiary part of the report deals with a method of flutter-speed calculation in which the aerodynamic terms are restricted to static derivatives only. No damping terms whatever are present in the equations of motion. The solution yields a boundary between constant amplitude and growing oscillations, which is regarded as the flutter critical condition. The method gives critical flutter speeds that agree surprisingly well with the experiments.

1. *Introduction.*—The idea of an aero-isoclinic wing was put forward by G. T. R. Hill¹. Briefly, it is a swept-back wing elastically designed so that the normal lifting loads do not affect the aerodynamic incidence. This aero-isoclinic property is obtained by adjustment of the flexural and torsional stiffnesses, their distributions, and the position of the locus of flexural centres so that the change of incidence produced by the torsion of the wing under air load is neutralised by that due to wing bending.

It was suggested by Hill that this type of wing would have an infinite divergence speed, and desirable characteristics with regard to flutter. A paper by Williams² primarily drawing attention to the possibility of a dynamic type of divergence, contained predictions of growing oscillations, and these results suggested that the flutter properties of an aero-isoclinic wing might be no better, or even worse, than those of a more conventional design. The simple method on which these predictions were based was however subject to uncertainty, since the sole aerodynamic derivatives involved referred to the static case.

The experiments of the present report were undertaken partly to gain some general knowledge of the flutter characteristics of an aero-isoclinic wing system, and partly to put to test the method on which the calculations of Williams were based. The model used was a practical interpretation of the simple aero-isoclinic system theoretically treated by Williams. It

* Published with the permission of the Director, National Physical Laboratory.

consisted of a rigid aerodynamic surface having the two essential freedoms, rotation about a swept-back axis, and rotation about a perpendicular axis at the root, these two rotations representing to a limited extent the twisting and bending of an actual wing. The two freedoms were spring-constrained and the stiffness ratio was adjusted to satisfy the isoclinic condition.

The results are not intended for quantitative application to a practical isoclinic wing, but rather to provide early experimental evidence to assist in the understanding of the problem.

2. List of Symbols Used

ϕ	Rotation about OX	} see Fig. 1
θ	Rotation about OY	
α	Aerodynamic incidence	
I_ϕ	Moment of inertia about OX	
I_θ	Moment of inertia about OY	
P	Product of inertia about OX, OY	
C_ϕ	Angular stiffness about OX	
C_θ	Angular stiffness about OY	
$M_\phi = k_\phi V^2 \alpha$	Aerodynamic moment about OX	
$M_\theta = k_\theta V^2 \alpha$	Aerodynamic moment about OY	
$f_\phi = p_\phi / 2\pi$	Uncoupled frequency of oscillation about OX	
$f_\theta = p_\theta / 2\pi$	Uncoupled frequency of oscillation about OY	
$f_c = p_c / 2\pi$	Flutter frequency	
$r = f_\phi / f_\theta$		
$q = P / I_\phi$		
$s = C_\phi / C_\theta$		
V	Air speed	
V_D	Divergence speed with freedom ϕ absent	
$n = V / V_D$		

PART I

Mainly Experimental

3. *Description of the System.*—The basic system is shown in Fig. 1. A rigid 45-deg swept-back wing ABCD, arranged close to a wall WW of the wind tunnel (National Physical Laboratory 4-ft No. 1) is able to rotate about an axis OY which lies at the mid-chord position. Axis OY can itself rotate about the perpendicular axis OX . The two degrees of freedom θ and ϕ , which to some extent may be regarded as representing torsion and flexure respectively, are spring-constrained without the introduction of a cross-stiffness. A photograph (Fig. 2) shows the apparatus set up away from the tunnel to illustrate the details. The wing was a portion of a non-swept rectangular aerofoil with a symmetrical profile, and having previously been used for derivative measurements it was conveniently mass-balanced about a mid-chord axis. The original aerofoil was modified to a swept-back wing by simply cutting off the ends at 45 deg. A

shaft rigidly clamped to the wing and projecting through the tunnel wall was supported by two ball-bearings to form the axis of rotation OY . These bearings were carried by a metal frame which was itself supported by two further ball-bearings rigidly attached to the tunnel wall and forming the second axis of rotation, OX . The metal frame was spring-constrained by 'earthed' springs S_ϕ , S_θ whose positions along the axis OY could be altered to provide a variation of C_ϕ , the angular stiffness about OX . Vertical rods R_1 , R_1 attached to the main shaft were connected to the frame by springs S_θ , S_θ which provide C_θ , the angular stiffness about OY . Initially springs S_θ , S_θ were chosen to give a convenient divergence speed V_D for the condition in which freedom ϕ was absent. Stiffness C_ϕ was then adjusted to make the system aero-isoclinic as explained in section 4.

Attachment of bob-weights to the rods R_1 , R_1 altered the ratio of the moments of inertia I_ϕ/I_θ , and thus altered the ratio r of the two uncoupled natural frequencies of the system. Horizontal rods also attached to the main shaft carried bob-weights to alter the product of inertia of the system about axis OX , OY . A further horizontal arm R_2 could be attached to the wing tip for a similar purpose. Since the stiffness C_θ was quite low, it would have been difficult to cancel out large unbalanced mass moments about axis OY by spring tensions, and conditions involving large products of inertia were obtained by two or more masses placed at different y positions and balanced about axis OY .

A small concave mirror M , attached to the main shaft as close as possible to the intersection of the axes OX and OY , threw, by means of a small plane mirror close above, a beam of light on to a large vertical screen (not shown in photograph). Displacements θ and ϕ of the system were then given respectively as vertical and horizontal displacements of the light spot.

No attempt was made to obtain moments of inertia, $I_\phi I_\theta$, consistent with the wing density of a practical wing. The inertias were in fact very large in comparison with the size of the wing, and a rough comparison of the inertia properties of the system with those of a practical wing may be made from the following consideration. A homogeneous wing of the same shape and size as the model, but with a wing density* $\sigma_w = 1.0$ lb/cu ft would have a moment of inertia I_ϕ of 0.15 slugs ft², which is approximately 0.1 of the value applicable to the model.

4. *The Aero-isoclinic Condition.*—For small displacements of the system, the incidence of the wing may be written,

$$\begin{aligned}\alpha &= \theta \cos \beta + \phi \sin \beta \\ &= (\theta + \phi)/\sqrt{2}, \quad \text{since } \beta = 45 \text{ deg.}\end{aligned}$$

It was convenient for the experiments to define the aero-isoclinic condition as follows. If the equilibrium position of the system in still air is (ϕ_0, θ_0) and the corresponding equilibrium position at an air speed V is (ϕ_v, θ_v) , then the stiffness ratio C_ϕ/C_θ is correctly adjusted to make the system aero-isoclinic when

$$\phi_0 + \theta_0 = \phi_v + \theta_v.$$

In the experiment ϕ and θ were directly observed as horizontal and vertical displacements of a spot of light on the screen, and the aero-isoclinic condition would have been satisfied when, with any alteration of air speed, the spot travelled along a line at 45 deg to the horizontal.

* 'Wing density' is defined as follows

$$\sigma_w = \text{wing mass}/(\text{wing area} \times \text{mean chord}).$$

It was found that $(C_\phi/C_\theta)_i$, the stiffness ratio required to satisfy the aero-isoclinic condition, depended both on the air speed and on the values of ϕ and θ . The aerofoil section of the wing had its maximum thickness close to the mid-chord position; this fact suggested that the dependence on air speed might be due to a chordwise movement of a separation of a laminar boundary layer resulting in a change of aerodynamic centre. Some improvement was in fact effected by attaching 'transition wires' at the mid-chord position and these were retained throughout the oscillatory tests.

Although a considerable amount of time was spent in investigating the dependence of the ratio $(C_\phi/C_\theta)_i$ on the values of ϕ and θ , no definite explanation could be found and it seems that the phenomenon can only be attributed to some asymmetry of the model or the airstream.

At an air speed of 30 ft sec $(C_\phi/C_\theta)_i$ appeared to be constant for displacements for which $\alpha > 2.0$ deg approximately and also constant for those for which $\alpha < -2.0$ deg and the following values of the aero-isoclinic stiffness ratio were obtained:

α	$(C_\phi/C_\theta)_i$
> 2.0 deg	10.6
< -2.0 deg	5.0

The stiffness ratio was finally adjusted to the value 7.77 (roughly the mean of the above values) to give an approximation to an aero-isoclinic condition. In view of the qualitative nature of the experiments this approximation was considered to be justified.

5. *Preliminary Measurements.*—The product of inertia of the system was initially brought to zero by adjustment of the masses on the horizontal arms. The experimental test for this condition was that no θ motion should occur when an impulse (a jerk by hand) was given to the ϕ freedom; this method although very simple provided a sensitive method of adjusting the position of the masses. The product of inertia for any subsequent condition was estimated from the additional masses and their positions. Initially, and after each addition of masses to rods R_1, R_1 , care was taken to see that no gravitational stiffness was present by balancing the system about OY when springs S_θ, S_θ were removed.

Angular stiffnesses C_ϕ and C_θ were measured by locking each freedom in turn with straining wires and by applying moments and measuring the deflections of the light spot on the screen.

The uncoupled natural frequencies f_ϕ, f_θ were measured by timing 10 free oscillations with the appropriate freedom locked. Quoted values of the inertias I_ϕ and I_θ were calculated from frequencies and stiffnesses.

6. *Critical Speed and Frequency Measurements.*—The divergence speed, V_D , appropriate to ϕ absent was determined by locking the ϕ freedom as explained above, and by raising the air speed until the system was in neutral equilibrium for small values of θ . This condition occurred at 45.4 ft/sec, and was quite critical to air speed.

Flutter critical speeds were measured by the usual method of finding the lowest air speed at which an oscillation of reasonable amplitude would be maintained. The flutter frequencies were low enough to allow stop-watch timing.

7. *Experimental Results.*—The flutter experiments consisted of two series of tests. The main series referred to the system with zero product of inertia, and flutter critical speeds and frequencies were measured for a range of values of I_θ whilst I_ϕ maintained approximately the same value. The second series referred to a product of inertia $P = -0.144$ slugs ft² (corresponding to a wing with forward mass-loading), and critical speeds and frequencies were again measured for a range of values of I_θ .

The complete experimental results are set out in Tables 1 and 2 which also give the values of the derived non-dimensional parameters r , n_c and q used by Williams. Fig. 3 gives the experimental results as graphs of n_c and $f_c/\sqrt{(f_\theta f_\phi)}$ plotted against r , and affords a comparison with calculated results.

With zero product of inertia the normal modes of vibration in still air consisted of one pure ϕ motion and one pure θ motion (still-air aerodynamic forces being neglected). With a finite product of inertia, the normal modes consisted of coupled ϕ and θ motion, and a possible normal mode is defined by

$$\phi + \theta = \text{const}$$

and since the incidence is constant during the oscillation, this mode may appropriately be termed isoclinic. In Part II an analysis leads to the conclusion that as the lower normal mode tends to become isoclinic, the flutter speed tends to become infinite.

Although no precise measurements of the normal modes were made, it was noticed during the experiments with a negative product of inertia that the lowest free oscillation in still air approximated to an isoclinic mode for all the chosen values of r , and that this approximation became even closer as the critical speed increased.

During the tests with a negative product of inertia, the air speed was raised above the divergence speed V_D and the peculiar characteristics of the system under these conditions is worthy of note. If the system was touched, or if during an oscillation it happened to hit against the amplitude stops, divergence was likely to occur since the aero-isoclinic property had been upset.

8. *Calculated Results.*—A systematic series of calculations was carried out using the theoretical method of Williams², which together with some amplification is dealt with in Part II. To provide a general picture, the smaller values of n_c given by equation (12) of Part II were computed for a range of r for $q = -0.075, -0.05, -0.01, 0$, and $+0.075$. These results are shown in Fig. 4.

For comparison with the experimental results a further set of calculations was made referring to $q = -0.06$ which is the mean of the values of q used in the experiments with a negative product of inertia. Theoretical values of the quantity $f_c/\sqrt{(f_\theta f_\phi)}$ were also computed for $q = 0, -0.06$.

The calculated results necessary for a comparison with experiment are shown in Fig. 3.

9. *Discussion of the Results.*—The agreement between the calculated and experimental results is sufficiently close to allow the general forms of both sets of results to be discussed at the same time.

The results clearly show that the aero-isoclinic property is not a sufficient condition for the elimination of flutter. No dynamic divergences were encountered and theory suggests that such an instability can never occur at a speed below the flutter speed. The flutter-speed curve of Fig. 3 shows that the critical speed decreases as the two natural frequencies of the system approach one another, and an increase in the frequency ratio f_θ/f_ϕ to a value above unity leads to a steep increase in the critical speed. As with conventional wings mass-loading forward of the flexural axis raises the critical speed.

The high equivalent wing density of the model is one of the factors that must be considered before any use is made of the experimental results to assist in the understanding of the flutter problem of a practical aero-isoclinic wing. As far as is known, there is no definite experimental evidence on the effect of a large increase in wing density on the flutter critical speed. Calculations made by Duncan, Lyon and Griffith^{3,4} for a normal cantilever wing show that the flutter critical speed decreases with an increase of wing density, and that it tends to an asymptotic value when the wing density becomes very large (*i.e.*, when σ_w much exceeds 1.0). This conclusion may however be open to some suspicion since the calculations were based on a set of constant derivative coefficients that may not be sufficiently accurate for dealing with cases of high wing density where the frequency parameter ω is likely to be low. However even in spite of lack of evidence, it is suggested that the present experimental results are qualitatively the same as those which would have been obtained with a lighter model. A justification for this view is provided by the good qualitative agreement that exists between the experimental results and those obtained theoretically by Houbolt⁵ for a system having a practical value for the wing density.

10. *Comparison between Experiment and Calculation.*—The reason for the apparently surprising agreement between experiment and a theory involving the drastic assumption of zero aerodynamic damping probably depends to a large extent on the high equivalent wing density and the low frequency parameter which this entails. Now in general as the frequency parameter tends to zero, the aerodynamic stiffnesses tend to their static values, and the aerodynamic damping forces tend to zero, and thus for low values of the frequency parameter it is not unreasonable that calculations neglecting damping and using static stiffnesses should give results in agreement with experiment. It has already been suggested that the present experimental results are qualitatively the same as those applicable to a system with a practical wing density. In view of the agreement between the experimental and calculated results, the above suggestion leads to the possibility that the method of calculation in which damping is neglected may be able to provide qualitative information on other flutter problems.

11. *Summary of Conclusions.*—(a) The experiments show that the aero-isoclinic condition is not sufficient to prevent flutter, and further that the critical speed may be low

(b) The flutter critical speed can be increased by forward mass-loading of the wing

(c) There is no indication that dynamic divergence will occur at a speed below the flutter critical speed

(d) The method of flutter-speed calculation in which the sole aerodynamic terms are static stiffness derivatives appears to give reasonable results for a system whose wing density is high.

PART II

An Analysis of the System

12. *In an Air Stream.*—The behaviour of the experimental system is investigated by the method of Williams².

The assumption is made that the aerodynamic moments M_ϕ and M_θ about axes OX and OY respectively are proportional to the instantaneous incidence of the wing and independent of the time rates of change of ϕ and θ , thus

$$M_\phi = k_\phi V^2 \alpha = k_\phi V^2 (\theta + \phi) / \sqrt{2}$$

$$M_\theta = k_\theta V^2 \alpha = k_\theta V^2 (\theta + \phi) / \sqrt{2}.$$

The equations of motion referred to axes OX and OY are then,

$$I_\phi \ddot{\phi} + C_\phi \dot{\phi} + P\ddot{\theta} = M_\phi = k_\phi V^2(\theta + \phi)/\sqrt{2} \quad \dots \quad (1)$$

$$I_\theta \ddot{\theta} + C_\theta \dot{\theta} + P\ddot{\phi} = M_\theta = k_\theta V^2(\theta + \phi)/\sqrt{2} \quad \dots \quad (2)$$

Let the divergence speed for the system with freedom ϕ absent be V_D , then

$$C_\theta = k_\theta V_D^2/\sqrt{2} \quad \dots \quad (3)$$

The aero-isoclinic condition is satisfied when there is no change of incidence with air speed. That is

$$0 = \sqrt{2}(\Delta\alpha) = \Delta\theta + \Delta\phi = (k_\theta/C_\theta + k_\phi/C_\phi)V^2\alpha$$

or
$$-k_\phi/k_\theta = C_\phi/C_\theta \quad \dots \quad (4)$$

By writing,

$$V/V_D = n$$

$$p_\phi = (C_\phi/I_\phi)^{1/2}$$

$$p_\theta = (C_\theta/I_\theta)^{1/2}$$

$$r = p_\phi/p_\theta$$

$$q = P/I_\phi$$

$$s = C_\phi/C_\theta$$

and by using equations (3) and (4), the equations of motion become,

$$\ddot{\phi} + (1 + n^2)r^2p_\theta^2\dot{\phi} + q\ddot{\theta} + n^2r^2p_\theta^2\theta = 0 \quad \dots \quad (5)$$

$$(qs/r^2)\ddot{\phi} - n^2p_\theta^2\dot{\phi} + \ddot{\theta} + (1 - n^2)p_\theta^2\theta = 0 \quad \dots \quad (6)$$

The solutions are of the form

$$\phi = \phi_0 e^{\lambda t}$$

$$\theta = \theta_0 e^{\lambda t}$$

where λ is given by the auxiliary equation

$$A\lambda^4 + B\lambda^2 + C = 0 \quad \dots \quad (7)$$

which yields

$$\lambda^2 = \frac{-B \pm \sqrt{B^2 - 4AC}}{2A} \quad \dots \quad (8)$$

where,

$$A = (1 - q^2s/r^2) \quad \dots \quad (9)$$

$$B = p_\theta^2[(1 - n^2) + r^2(1 + n^2) - n^2q(s - 1)] \quad \dots \quad (10)$$

$$C = r^2p_\theta^4 \quad \dots \quad (11)$$

Since $(I_\phi I_\theta - P^2) \ll 0$, A can be shown to be positive, whilst C is necessarily positive, and thus the roots λ^2 of equation (7) will be both real and positive, or both real and negative or a complex pair. When λ^2 and λ are written in the general form

$$\lambda^2 = a + ib$$

$$\lambda = c + id$$

the conditions under which the various types of root exist may be seen from the following table in which the suffixed symbols represent positive quantities:

n	B	$B^2 - 4AC$	λ^2	λ	Physical interpretation
increasing 	> 0	> 0	$-a_1 \longrightarrow$ $-a_2 \longrightarrow$	$\pm id_1$ $\pm id_2$	two maintained oscillations
	> 0	< 0	$-a_1 \pm ib_1$	$\left\{ \begin{array}{l} c_1 \pm id_1 \\ -c_1 \pm id_1 \end{array} \right\}$	one growing oscillation
	< 0	< 0	$a_1 \pm ib_1$		$\left\{ \begin{array}{l} c_1 \pm id_1 \\ -c_1 \pm id_1 \end{array} \right\}$
	< 0	> 0	$+a_1 \longrightarrow$ $+a_2 \longrightarrow$	$\pm c_1$ $\pm c_2$	two divergences + two subsidences

The divergences referred to in the above table do not correspond to the usual static divergences which occur with a non-aero-isoclinic system when an aerodynamic stiffness neutralises an elastic stiffness. The present type may be termed dynamic divergences as suggested by Williams.

The condition $B^2 - 4AC = 0$, $B > 0$ represents a change from stable oscillations to a growing oscillation, and this is regarded as the condition for incipient flutter.

Substitution of the expressions for A , B and C in the condition

$$B^2 - 4AC = 0$$

leads to the following expression for n_c , corresponding to the critical air speed:

$$n_c^2 = \frac{(r^2 + 1) \pm 2\sqrt{[r^2(1 - q^2s/r^2)]}}{(1 - r^2) + q(s - 1)} \quad \dots \quad (12)$$

where the smaller root refers to the change from stable oscillations to a growing oscillation (the flutter critical speed), and the larger root to a change from a growing oscillation to a divergence (the critical speed for a dynamic divergence). The flutter speed is thus always less than the speed at which dynamic divergence occurs.

Since $B^2 - 4AC = 0$ at the flutter critical speed the flutter frequency f_c is from equation (8) given by

$$4\pi^2 f_c^2 = \lambda^2 = -\frac{B}{2A} = \sqrt{\left(\frac{C}{A}\right)}$$

or

$$f_c = (f_\theta f_\phi)^{1/2} / (1 - q^2s/r^2)^{1/4} \quad \dots \quad (13)$$

For the particular case where the product of inertia is zero (i.e., $q = 0$) the critical speed boundaries are given by

$$n_c^2 = \frac{1 - r}{1 + r} \text{ or } \frac{1 + r}{1 - r}$$

and

$$r = 1$$

whilst the flutter frequency is

$$f_c = (f_0 f_\phi)^{1/2}.$$

Fig. 5 illustrates the stability of the system as a graph of n plotted against r for a typical condition $q \neq 0$, whilst Fig. 6 corresponds to the particular case $q = 0$.

It is seen that the results of the above analysis do not involve the position of the axis OY explicitly. The expressions for the critical speed parameter n_c , and frequency given by equations (12) and (13) are in fact valid for any chordwise position of the axis OY provided that the system is aero-isoclinic; it has, however, tacitly been assumed that OY lies behind the aerodynamic centre of the aerofoil section, so that k_θ is positive and thus a real divergence speed V_D exists.

Then with this proviso, it is seen that the system is stable for all values of n , when

$$(1 - r^2) + q(s - 1) < 0. \quad \dots \dots \dots (14)$$

13. *In Still Air.*—The equations of motion of the system in still air are, if all aerodynamic forces are neglected,

$$\left. \begin{aligned} I_\phi \ddot{\phi} + C_\phi \dot{\phi} + P\ddot{\theta} &= 0 \\ P\ddot{\phi} + I_\theta \ddot{\theta} + C_\theta \dot{\theta} &= 0 \end{aligned} \right\} \dots \dots \dots (15)$$

The solution is of the form

$$\begin{aligned} \phi &= \Phi \sin pt \\ \theta &= \Theta \sin pt \end{aligned}$$

and no restriction is placed on the sign of Φ and Θ . By substitution in the original equations we have

$$R = \frac{Pp^2}{C_\phi - I_\phi p^2} = \frac{C_\theta - I_\theta p^2}{Pp^2} \quad \dots \dots \dots (16)$$

where $R = \Phi/\Theta$, and defines the mode of vibration.

By eliminating p from equations (16) the following quadratic in R is obtained,

$$R^2 + R(I_\theta/P - I_\phi C_\theta/PC_\phi) - C_\theta/C_\phi = 0$$

or
$$R^2 + R(r^2 - 1)/sq - 1/s = 0. \quad \dots \dots \dots (17)$$

Now for the system under consideration, the normal modes are completely defined by the positions of the nodal lines. Since the displacement z at any point x, y of the system is given by

$$z = \phi y + \theta x$$

the equation of a nodal line is

$$0 = z = \Phi y + \Theta x$$

or

$$x/y = -\Phi/\Theta = -R.$$

Clearly since all the nodal lines pass through the origin O the nodal line, and thus the normal mode, are sufficiently defined by the angle γ that the line makes with axis OY (see Fig. 7) where

$$\tan \gamma = -R.$$

The normal mode defined by $R_1 = -1$ does not involve a change of incidence α , and may be described as an isoclinic mode. Now the condition that one of the roots of equation (17) is -1 is

$$(1 - r^2) + q(s - 1) = 0$$

and this has been shown to be the condition that the flutter speed shall tend to ∞ (see equation (14)).

14. *Correlation between Nodal Line and Flutter.*—It has been shown in section 12 that there will be no real critical speed provided that

$$(1 - r^2) + q(s - 1) < 0.$$

This inequality yields the following condition for the product of inertia coefficient q for complete absence of flutter:

$$q < \frac{r^2 - 1}{s - 1}.$$

Now the ranges of the roots R_1 and R_2 of equation (17) for the range*

$$\frac{r^2 - 1}{s - 1} > q > -\infty$$

are, when $s > 1$, given as follows:

(a) When $r < 1$

$$-1/\sqrt{s} > R_1 > -1$$

$$1/\sqrt{s} > R_2 > 1/s$$

(b) When $r > 1$

$$\sqrt{s} > 1/R_1 > -1$$

$$1/s > R_2 > -1/\sqrt{s}.$$

* The smaller limit of q is in practice $-r/\sqrt{s}$.

From these results Figs. 7a and 7b have been plotted to show the regions for the nodal lines for which theoretically no finite flutter speed exists.

REFERENCES

- | <i>No.</i> | <i>Author</i> | <i>Title, etc.</i> |
|------------|----------------------------------------|-----------------------------------------------------------------------------------------------------------------------------------------------|
| 1 | G. T. R. Hill | A proposal for a solution to the low-speed stability and high-speed aero-elastic problems of tailless aircraft. A.R.C. 11,424. (Unpublished.) |
| 2 | D. Williams | A simplified treatment of a fixed-root swept wing built on Hill's isoclinic principle. R. & M. 2870. January, 1951. |
| 3 | W. J. Duncan and H. M. Lyon .. | Calculated flexural-torsional flutter characteristics of some typical cantilever wings. R. & M. 1782. April, 1937. |
| 4 | W. J. Duncan and C. L. T. Griffiths .. | The influence of wing taper on the flutter of cantilever wings. R. & M. 1869. July, 1939. |
| 5 | John C. Houbolt | Aeroelastic behaviour of the aero-isoclinic wing under sudden loads. A.R.C. 12,521. June, 1949. (Unpublished.) |
-

TABLE 1

Experimental Results with Product of Inertia Zero

f_0 c/sec	f_ϕ c/sec	$r \equiv f_\phi/f_0$	I_0 slugs ft ²	I_ϕ slugs ft ²	P slugs ft ²	V_c ft/sec	f_c c/sec	$\frac{\omega_c}{\equiv 2\pi f_c/V_c}$	$n \equiv V_c/V_D$	$f_c/\sqrt{(f_0 f_\phi)}$
1.316	0.417	0.317	0.016	1.28	0	31.3	0.943	0.091	0.690	1.27
1.075	0.415	0.386	0.025	1.29	0	29.0 ₅	0.806	0.098	0.640	1.21
0.820	0.412	0.503	0.043	1.31	0	25.9	0.662	0.110	0.571	1.14
0.676	0.410	0.607	0.063	1.32	0	21.6	0.583	0.132	0.475	1.11
0.572	0.405	0.708	0.087	1.36	0	17.8 ₅	0.516	0.159	0.393	1.07
0.525	0.403	0.768	0.104	1.37	0	16.6	0.486	0.171	0.367	1.06
0.503	0.402	0.799	0.113	1.38	0	14.9 ₅	0.473	0.190	0.329	1.05
0.488	0.401 ₅	0.823	0.120	1.38	0	14.3	0.459	0.199	0.314	1.04
0.451	0.396	0.870	0.141	1.42	0	11.6	0.434	0.246	0.254	1.03
0.459	0.400	0.872	0.136	1.39	0	12.6	0.442 ₅	0.226	0.278	1.03
0.442 ₅	0.398 ₅	0.900	0.146	1.40	0	11.2	0.429	0.254	0.247	1.02
0.431	0.397	0.921	0.154	1.41	0	11.1	0.422	0.256	0.244	1.02
0.419 ₅	0.393 ₅	0.939	0.163	1.44	0	9.8	0.414	0.290	0.216	1.02
0.414	0.396	0.956	0.167	1.42	0	9.4	0.411	0.304	0.206	1.02
0.405	0.394	0.972	0.174	1.43	0	10.3	0.402	0.276	0.227	1.01
0.400	0.394	0.984	0.177	1.43	0	12.7 ₅	0.402	0.223	0.281	1.01
0.396	0.394	0.995	0.182	1.43	0	16.3	0.396	0.175	0.359	1.00
0.387 ₅	0.393	1.015	0.190	1.44	0	25.1	0.382	0.113	0.552	0.98
0.383	0.392	1.022	0.195	1.45	0	27.3	0.370 ₅	0.104	0.601	0.96
0.373	0.390	1.047	0.206	1.46	0	36.5	0.351	0.078	0.804	0.92
0.343	0.385	1.121	0.243	1.50	0	67.8 ₅	—	—	1.495	—

TABLE 2

Experimental Results with a Negative Product of Inertia

f_0 c/sec	f_ϕ c/sec	$r \equiv f_\phi/f_0$	I_0 slugs ft ²	I_ϕ slugs ft ²	P slugs ft ²	V_c ft/sec	f_c c/sec	$\frac{\omega_c}{2\pi f_c c/V_c}$	$n \equiv V_c/V_D$	$f_c/\sqrt{(f_0 f_\phi)}$	q
0.575	0.307	0.534	0.087	2.36	-0.144	51.2	0.427	0.056	1.13	1.02	-0.061
0.570	0.309	0.541	0.088	2.34	-0.144	50.5	0.415	0.023	1.11	0.99	-0.062
0.520	0.305	0.589	0.106	2.39	-0.144	51.4	0.404	0.022	1.13	1.01	-0.060
0.459	0.302	0.658	0.136	2.44	-0.144	49.7	0.376	0.022	1.10	1.01	-0.059
0.429	0.303	0.707	0.156	2.42	-0.144	54.6	0.374	0.019	1.20	1.04	-0.059
0.379	0.301	0.794	0.201	2.40	-0.144	>69.4	—	—	>1.53	—	-0.060

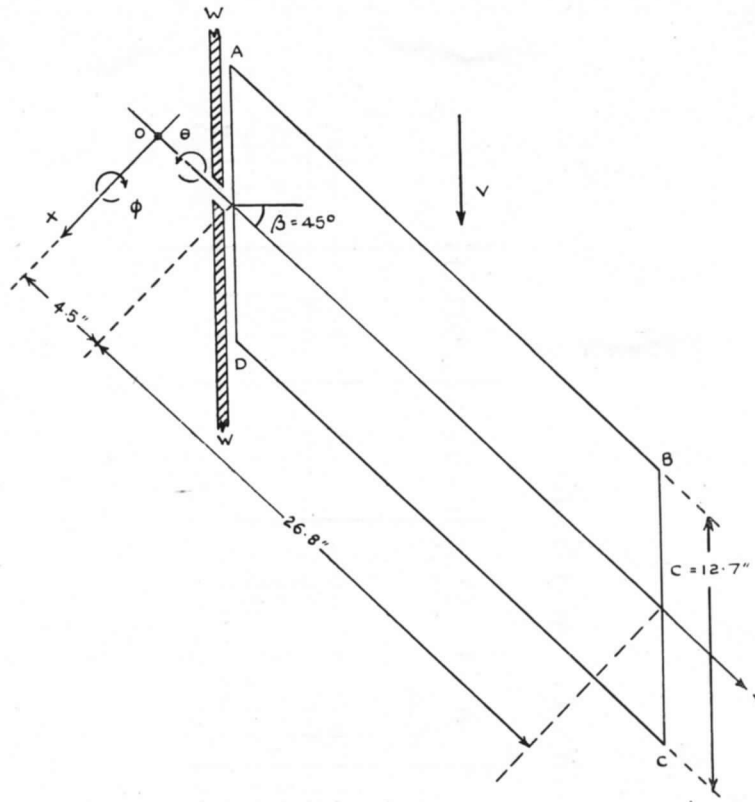


FIG. 1. The basic system.

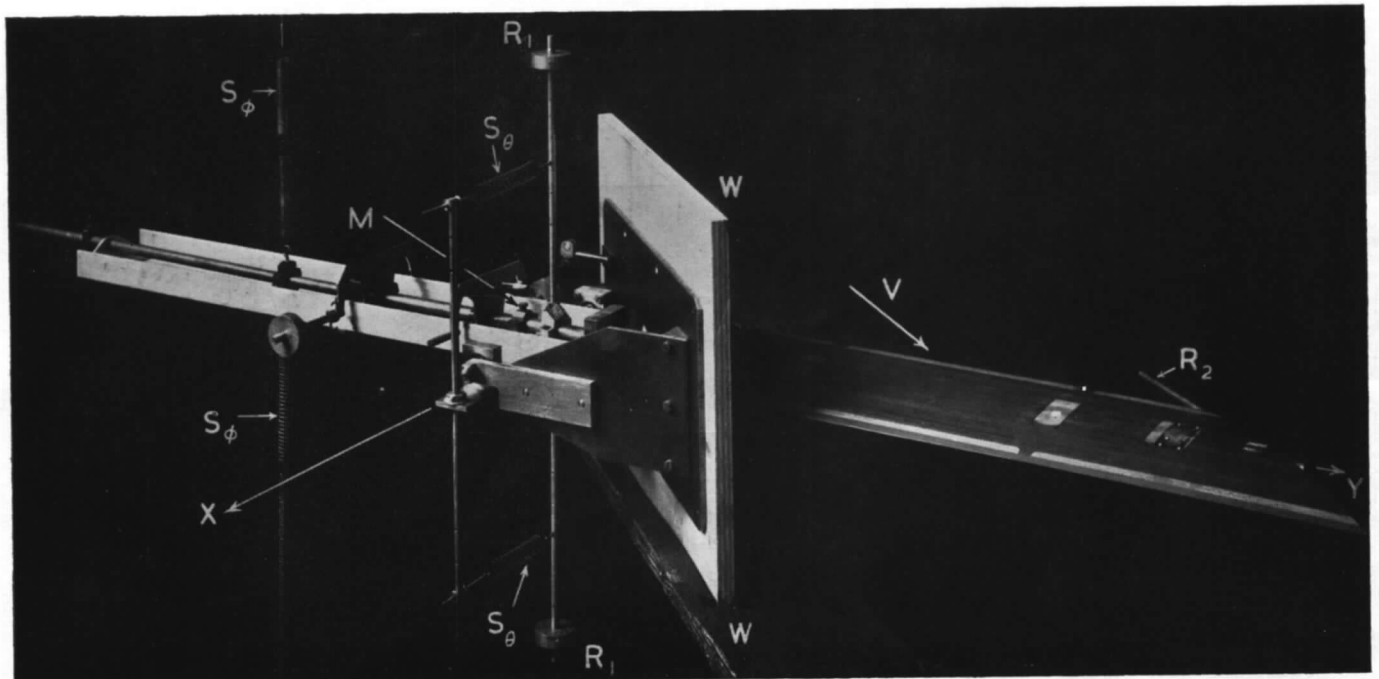


FIG. 2.

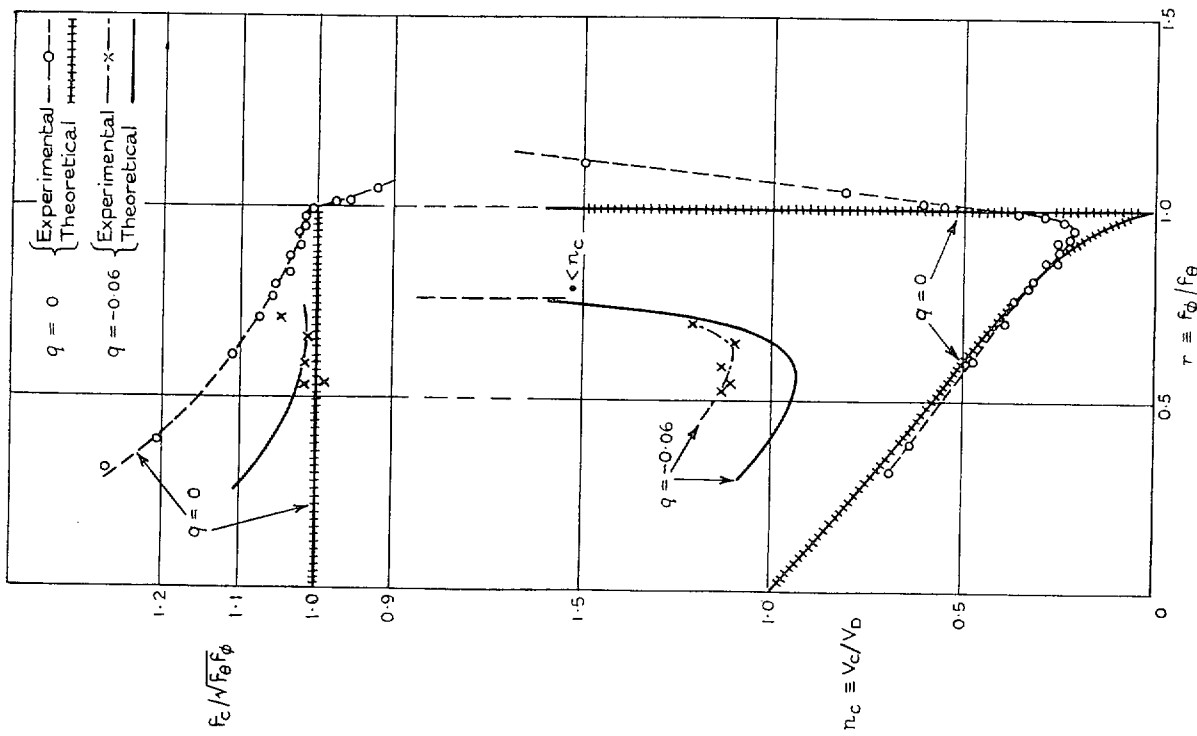


FIG. 3. Experimental and theoretical critical speeds and frequencies.

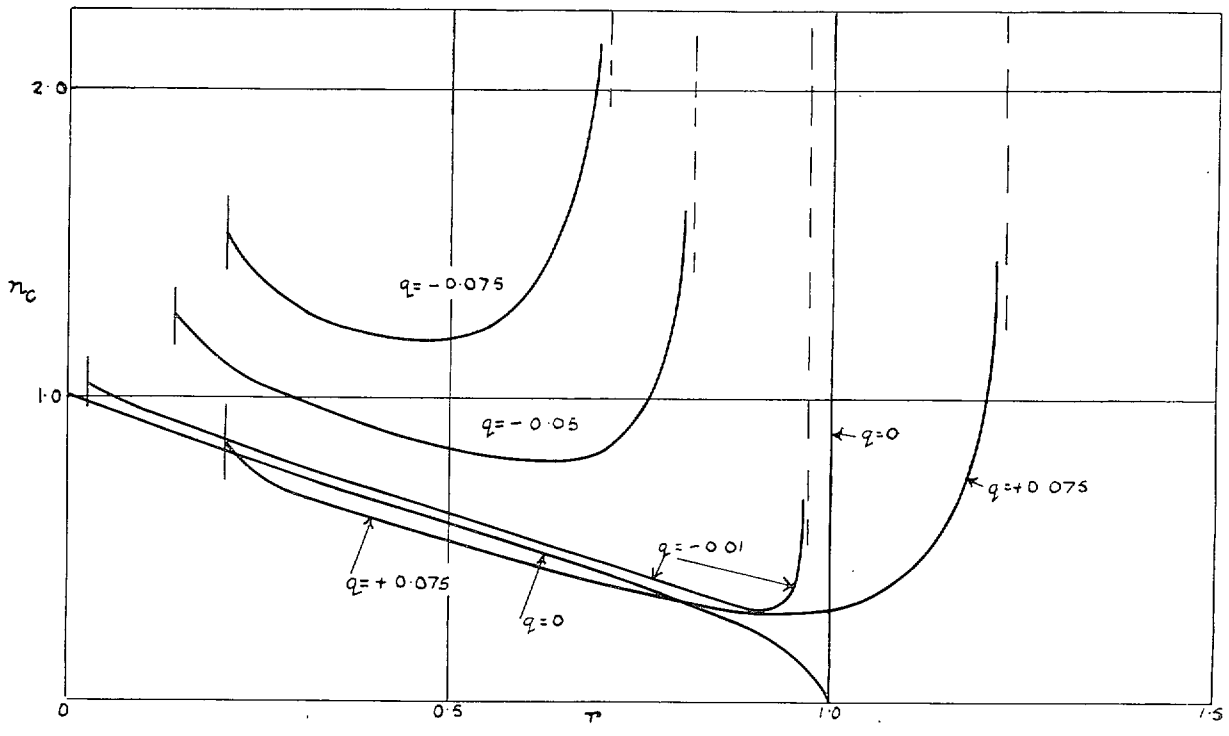


FIG. 4. Theoretical variation of n_c with τ for various values of q .

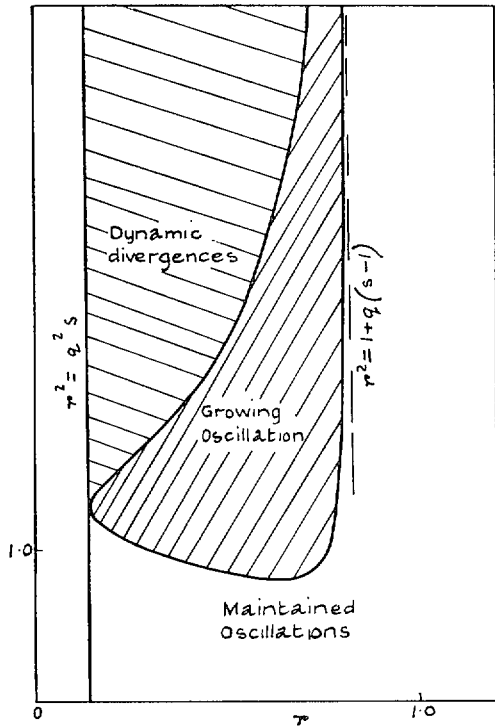


FIG. 5. The theoretical stability boundaries for general case $q \neq 0$.

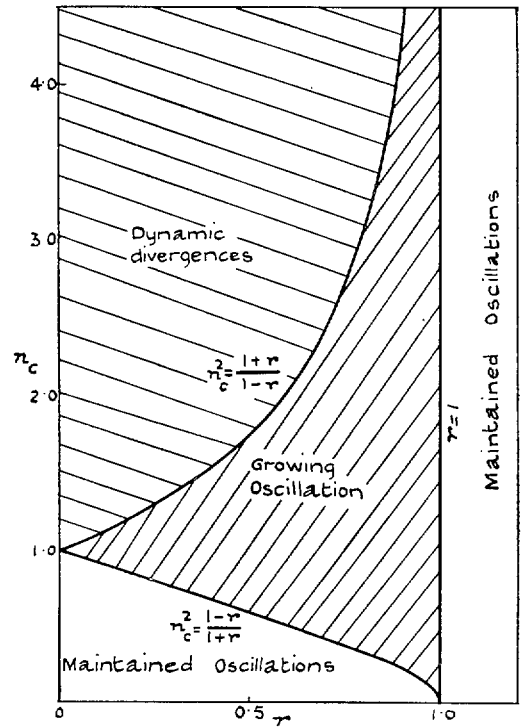


FIG. 6. The theoretical stability boundaries for $q = 0$.

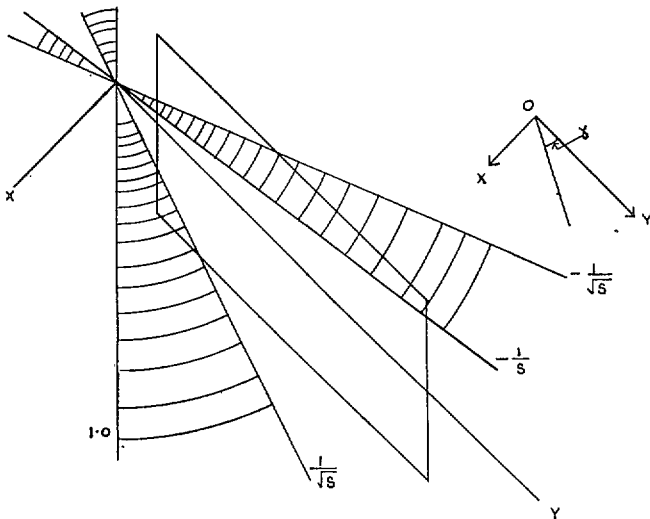


FIG 7a. $r < 1$.

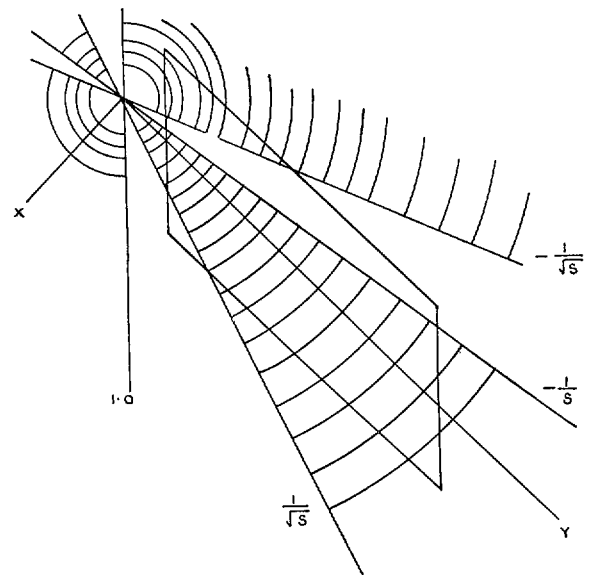


FIG. 7b. $r > 1$.

FIGS. 7a and 7b. Theoretical correlation between position of nodal line and possibility of flutter. The system is flutter free when nodal lines lie within shaded areas ($s = 7.77$). Values of x/y indicated against lines.

Publications of the Aeronautical Research Council

ANNUAL TECHNICAL REPORTS OF THE AERONAUTICAL RESEARCH COUNCIL (BOUND VOLUMES)—

- 1939 Vol. I. Aerodynamics General, Performance, Airscrews, Engines. 50s. (51s. 9d.)
Vol. II. Stability and Control, Flutter and Vibration, Instruments, Structures, Seaplanes, etc. 63s. (64s. 9d.)
- 1940 Aero and Hydrodynamics, Aerofoils, Airscrews, Engines, Flutter, Icing, Stability and Control, Structures, and a miscellaneous section. 50s. (51s. 9d.)
- 1941 Aero and Hydrodynamics, Aerofoils, Airscrews, Engines, Flutter, Stability and Control, Structures. 63s. (64s. 9d.)
- 1942 Vol. I. Aero and Hydrodynamics, Aerofoils, Airscrews, Engines. 75s. (76s. 9d.)
Vol. II. Noise, Parachutes, Stability and Control, Structures, Vibration, Wind Tunnels. 47s. 6d. (49s. 3d.)
- 1943 Vol. I. Aerodynamics, Aerofoils, Airscrews. 80s. (81s. 9d.)
Vol. II. Engines, Flutter, Materials, Parachutes, Performance, Stability and Control, Structures. 90s. (92s. 6d.)
- 1944 Vol. I. Aero and Hydrodynamics, Aerofoils, Aircraft, Airscrews, Controls. 84s. (86s. 3d.)
Vol. II. Flutter and Vibration, Materials, Miscellaneous, Navigation, Parachutes, Performance, Plates and Panels, Stability, Structures, Test Equipment, Wind Tunnels. 84s. (86s. 3d.)
- 1945 Vol. I. Aero and Aerodynamics, Aerofoils. 130s. (132s. 6d.)
Vol. II. Aircraft, Airscrews, Controls. 130s. (132s. 6d.)
Vol. III. Flutter and Vibration, Instruments, Miscellaneous, Parachutes, Plates and Panels, Propulsion. 130s. (132s. 3d.)
Vol. IV. Stability, Structures, Wind Tunnels, Wind Tunnel Technique. 130s. (132s. 3d.)

ANNUAL REPORTS OF THE AERONAUTICAL RESEARCH COUNCIL—

1937	2s. (2s. 2d.)	1938	1s. 6d. (1s. 8d.)
1939-48	3s. (3s. 3d.)		

INDEX TO ALL REPORTS AND MEMORANDA PUBLISHED IN THE ANNUAL TECHNICAL REPORTS, AND SEPARATELY—

April, 1950 R. & M. No. 2600 2s. 6d. (2s. 8d.)

AUTHOR INDEX TO ALL REPORTS AND MEMORANDA OF THE AERONAUTICAL RESEARCH COUNCIL—

1909-January, 1954 R. & M. No. 2570 15s. (15s. 6d.)

INDEXES TO THE TECHNICAL REPORTS OF THE AERONAUTICAL RESEARCH COUNCIL—

December 1, 1936 — June 30, 1939	R. & M. No. 1850 1s. 3d. (1s. 5d.)
July 1, 1939 — June 30, 1945	R. & M. No. 1950 1s. (1s. 2d.)
July 1, 1945 — June 30, 1946	R. & M. No. 2050 1s. (1s. 2d.)
July 1, 1946 — December 31, 1946	R. & M. No. 2150 1s. 3d. (1s. 2d.)
January 1, 1947 — June 30, 1947	R. & M. No. 2250 1s. 3d. (1s. 2d.)

PUBLISHED REPORTS AND MEMORANDA OF THE AERONAUTICAL RESEARCH COUNCIL—

Between Nos. 2251-2349	R. & M. No. 2350 1s. 9d. (1s. 11d.)
Between Nos. 2351-2449	R. & M. No. 2450 2s. (2s. 2d.)
Between Nos. 2451-2549	R. & M. No. 2550 2s. 6d. (2s. 2d.)
Between Nos. 2551-2649	R. & M. No. 2650 2s. 6d. (2s. 2d.)

Prices in brackets include postage

HER MAJESTY'S STATIONERY OFFICE

York House, Kingsway, London, W.C.2; 423 Oxford Street, London, W.1 (Post Orders: P.O. Box 569, London, S.E.1);
13a Castle Street, Edinburgh 2; 39 King Street, Manchester 2; 2 Edmund Street, Birmingham 3; 109 St. Mary Street,
Cardiff; Tower Lane, Bristol 1; 80 Chichester Street, Belfast or through any bookseller

S.O. Code No. 23-2869